Pergamon

Int. J. Heat Mass Transfer. Vol. 38, No. 2, pp. 219–231, 1995

0017-9310/95 $9.50+0.00

0017-9310(94)00156-1

Transient conjugate free convection due to a vertical plate in a porous medium

MICHAEL VYNNYCKY and SHIGEO KIMURA

Tohoku National Industrial Research Institute, Agency of Industrial Science and Technology, Ministry of International Trade and Industry, Nigatake, 4-2-1, Miyagino-Ku, Sendai, 983, Japan

(*Received* 7 *March* 1994 *and in final form* 27 *May* 1994)

Abstract—The problem of two-dimensional transient conjugate free convection due to a vertical plate of finite extent adjacent to a semi-infinite porous medium is investigated both analytically and numerically. In view of the number of nondimensional parameters present in the formulation, namely the Rayleigh number, Ra, the thermal conductivity and diffusivity ratios, k and α, respectively, between the plate and the porous medium, the heat capacity ratio, γ, for the porous medium and the plate aspect ratio, λ, a one-dimensional formulation is used to identify two parameter regimes, $Ra \gg 1$ and $\Gamma\ (=\gamma\alpha) \ll Ra$, and $\Gamma \gg 1$ and $Ra \ll \Gamma$, for which analytical solutions may be found; these are subsequently seen to compare favourably with computed solutions, also presented here, to the time-dependent governing heat and momentum equations. For the first of the parameter regimes mentioned above, the transient process is seen to develop towards the steady-state solution obtained by the same authors elsewhere.

1. INTRODUCTION

The problem of natural convection due to a heated vertical plate of finite extent placed adjacent to a semi-infinite porous medium provides one of the most basic scenarios for free convection, and is thus of considerable practical and theoretical interest. In recent years, in order to take account of physical reality, there has been a tendency to move away from considering idealised problems in which the plate is considered infinitesimally thin [1, 2], but instead to take account of the so-called conjugate effects which arise due to the finite thickness of the plate. In particular, papers by Vynnycky and Kimura [3, 4] have elucidated the steady-state problem for both the cases when the semi-infinite medium is either porous or fluid. Common to both works was the derivation of an approximate formula which predicts the average temperature and average Nusselt number at the conjugate boundary for high values of the Rayleigh number and which may be applied for a wide range of values of the thermal conductivity ratio, k, and plate aspect ratio, λ; furthermore, similar results have been obtained for the cases where conjugate free convection is due to a heated cylinder [5, 6] and a heated sphere [7].

As regards transient natural convection, some work has been carried out for the situation where the heated plate is thin: for example, Johnson and Cheng [8] considered all the possible similarity solutions that might arise in boundary-layer flow past such a plate, whilst Ingham and Brown [9] and Ingham *et al.* [10] investigated the effects, respectively, of suddenly heating and cooling a vertical plate in a porous medium. However, to the best of the authors' knowledge, there has been little investigation of time-dependent conjugate effects, despite the fact that, in reality, transient convection might be expected to be a precursor to steady convection and that the heated plate is not infinitesimally thin; it is to this, therefore, that this paper is addressed. In what follows, we make use of the work of Vynnycky and Kimura [3] to demonstrate the flow development with time. In Section 2, we formulate mathematically the problem of flow due to a vertical plate, initially at ambient temperature, one of whose sides is thereafter held fixed at a temperature greater than ambient. In Section 3, it is shown that the momentum and heat equations of Section 2 may be simplified, in certain cases, to obtain a problem which is much more tractable than the solution of the full equations; in particular, we demonstrate how our derived time-dependent equations reduce to the time-independent limit elucidated by Vynnycky and Kimura [3]. In Section 4, we present a full numerical solution to the governing equations, concentrating in particular on a comparison with the analytical results of Section 3 and on demonstrating the importance of the Rayleigh number, Ra, and Γ, the product of the ratio of heat capacity, γ, of the saturated porous medium to that of the fluid and the ratio of the thermal diffusivities (α_f/α_s) of the two media in influencing the flow. Finally, in Section 5 we draw conclusions.

2. MATHEMATICAL FORMULATION

Consider unsteady free convective flow due to a rectangular plate occupying the region $-a \leqslant x \leqslant 0$, $-b/2 \leqslant y \leqslant b/2$, adjacent to a semi-infinite fluid-saturated porous medium ($x > 0$, $-\infty \leqslant y \leqslant \infty$) (Fig. 1); initially, the whole system is at a temperature, T_∞,

NOMENCLATURE

a	thickness of the conducting plate
b	length of the conducting plate
g	acceleration due to gravity
k_f	effective thermal conductivity of the porous medium
k_s	thermal conductivity of the plate
k	thermal conductivity ratio, k_s/k_f
K	permeability of the porous medium
$\overline{Nu}_b$	dimensionless average Nusselt number at the conjugate boundary
$\overline{Nu}_w$	dimensionless average Nusselt number at the heated wall
Ra	Rayleigh number for the porous medium, $Kg\beta(T_c - T_\infty)b/\alpha_f\nu$
t	time variable
T_c	constant temperature of heated side of plate
T_∞	constant temperature of ambient fluid
x	horizontal coordinate
y	vertical coordinate
u, v	dimensionless velocity components along (x, y) axes
X_∞	size of computational domain in x-direction
Y_∞	size of computational domain in y-direction.

Greek symbols

α_f	thermal diffusivity of the porous medium
α_s	thermal diffusivity of the solid
α	thermal diffusivity ratio, α_s/α_f
β	coefficient of thermal expansion
γ	the ratio of heat capacity of saturated porous medium to that of fluid
Γ	dimensionless parameter, $\gamma\alpha_f/\alpha_s$
δ	boundary-layer thickness
θ_s	dimensionless temperature in the solid
θ_f	dimensionless temperature in the porous medium
$\bar{\theta}_b$	dimensionless average conjugate boundary temperature
$\Delta\theta$	temperature increment
λ	aspect ratio, a/b
ν	kinematic viscosity
ψ	dimensionless streamfunction
$\Delta\psi$	streamline increment.

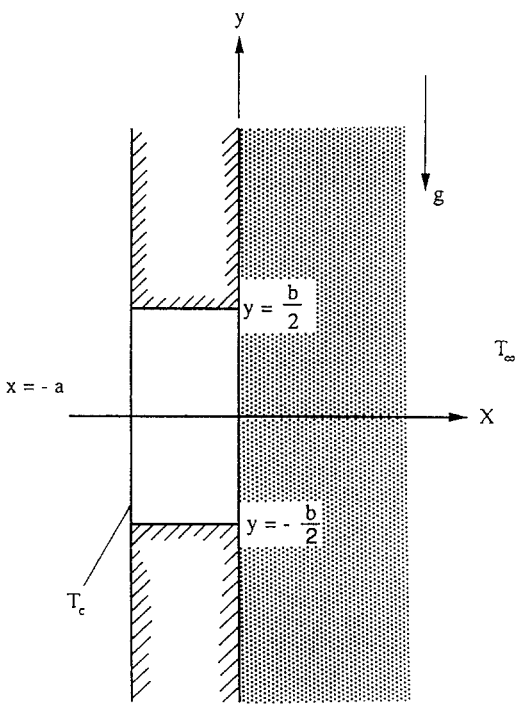

Fig. 1. Sketch of geometry for natural convection.

but subsequently the left-hand side of the plate is instantaneously raised to, and held at, a uniform temperature T_c ($> T_\infty$). The sides of the plate, $y = \pm b/2$ are insulated, whilst, for the porous medium, there is no heat flux and no normal outflow across $x = 0$, $|y| > b/2$; in addition, for $x = 0$, $|y| < b/2$, we expect both continuity of temperature and heat flux. Assuming that the porous medium is isotropic and homogeneous and that the fluid is incompressible, we invoke the Boussinesq–Darcy approximation to obtain the equations of continuity:

$$\frac{\partial u}{\partial x} + \frac{\partial v}{\partial y} = 0, \tag{1}$$

and momentum:

$$\frac{\partial u}{\partial y} - \frac{\partial v}{\partial x} = -\frac{g\beta K}{\nu}\frac{\partial T_f}{\partial x}, \tag{2}$$

the equation of energy in the fluid-porous medium:

$$\gamma\frac{\partial T_f}{\partial t} + u\frac{\partial T_f}{\partial x} + v\frac{\partial T_f}{\partial y} = \alpha_f\left(\frac{\partial^2 T_f}{\partial x^2} + \frac{\partial^2 T_f}{\partial y^2}\right), \tag{3}$$

and the equation of the heat transfer inside the solid plate:

$$\frac{\partial T_s}{\partial t} = \alpha_s\nabla^2 T_s, \tag{4}$$

where (u, v) are the velocity components in the (x, y) directions, T_f and T_s are the temperatures of the fluid-saturated porous medium and the solid plate, respectively, and the physical constants g, β, ν, K, α_f, α_s and γ

(and later k_s and k_f) are as given in the Nomenclature. Equations (1)–(4) are subject to the following boundary conditions:

$$u = 0 \quad \text{on} \quad x = 0, \tag{5}$$

$$T_s = T_f \quad k_f \frac{\partial T_f}{\partial x} = k_s \frac{\partial T_s}{\partial x} \quad \text{on} \quad x = 0 \quad |y| \leqslant \frac{b}{2}, \tag{6}$$

$$\frac{\partial T_f}{\partial x} = 0 \quad \text{on} \quad x = 0 \quad |y| > \frac{b}{2}, \tag{7}$$

$$T_s = T_c \quad \text{on} \quad x = -a \quad |y| \leqslant \frac{b}{2}, \tag{8}$$

$$\frac{\partial T_s}{\partial y} = 0 \quad \text{on} \quad y = \pm \frac{b}{2} \quad -a \leqslant x \leqslant 0, \tag{9}$$

$$T_f \to T_\infty \quad \text{as} \quad x \to \infty \quad y \to \pm\infty, \tag{10}$$

$$v \to 0 \quad \text{as} \quad x \to \infty, \tag{11}$$

$$u \to 0 \quad \text{as} \quad y \to \pm\infty. \tag{12}$$

Furthermore, we have the initial conditions:

$$T_s(x, y, 0) = T_\infty \quad \text{for} \quad -a \leqslant x \leqslant 0 \quad |y| < \frac{b}{2}, \tag{13}$$

$$T_f(x, y, 0) = T_\infty \quad \text{for} \quad x \geqslant 0 \quad -\infty < y < \infty, \tag{14}$$

$$u = v = 0 \quad \text{for} \quad x \geqslant 0, \quad -\infty < y < \infty. \tag{15}$$

By employing the following non-dimensionalisation,

$$x^* = \frac{x}{b} \quad y^* = \frac{y}{b} \quad t^* = \frac{\alpha_s t}{b^2} \quad u^* = \frac{bu}{\alpha_f}$$

$$v^* = \frac{bv}{\alpha_f} \quad \theta_s^* = \frac{T_s - T_\infty}{T_c - T_\infty} \quad \theta_f^* = \frac{T_f - T_\infty}{T_c - T_\infty},$$

subsequently dropping the asterisks and then defining the dimensionless stream function by:

$$u = \frac{\partial \psi}{\partial y} \quad v = -\frac{\partial \psi}{\partial x},$$

we arrive at:

$$\nabla^2 \psi = -Ra \frac{\partial \theta_f}{\partial x}, \tag{16}$$

$$\Gamma \frac{\partial \theta_f}{\partial t} + \frac{\partial \psi}{\partial y}\frac{\partial \theta_f}{\partial x} - \frac{\partial \psi}{\partial x}\frac{\partial \theta_f}{\partial y} = \nabla^2 \theta_f, \tag{17}$$

$$\frac{\partial \theta_s}{\partial t} = \nabla^2 \theta_s, \tag{18}$$

subject to:

$$\psi = 0 \quad \text{on} \quad x = 0, \tag{19}$$

$$\frac{\partial \theta_f}{\partial x} = 0 \quad \text{on} \quad x = 0 \quad |y| > \tfrac{1}{2}, \tag{20}$$

$$\theta_s = 1 \quad \text{on} \quad x = -\lambda \quad |y| \leqslant \tfrac{1}{2}, \tag{21}$$

$$\theta_s = \theta_f \quad \text{on} \quad x = 0 \quad |y| \leqslant \tfrac{1}{2}, \tag{22}$$

$$k \frac{\partial \theta_s}{\partial x} = \frac{\partial \theta_f}{\partial x} \quad \text{on} \quad x = 0 \quad |y| \leqslant \tfrac{1}{2}, \tag{23}$$

$$\frac{\partial \theta_s}{\partial y} = 0 \quad \text{on} \quad y = \pm \tfrac{1}{2} \quad -\lambda \leqslant x \leqslant 0, \tag{24}$$

$$\theta_f \to 0 \quad \frac{\partial \psi}{\partial x} \to 0 \quad \text{as} \quad x \to \infty, \tag{25}$$

$$\theta_f \to 0 \quad \frac{\partial \psi}{\partial y} \to 0 \quad \text{as} \quad y \to \pm\infty, \tag{26}$$

$$\theta_s(x, y, 0) = 0 \quad \text{for} \quad -\lambda \leqslant x \leqslant 0 \quad |y| < \tfrac{1}{2}, \tag{27}$$

$$\theta_f(x, y, 0) = 0 \quad \text{for} \quad x \geqslant 0 \quad -\infty < y < \infty, \tag{28}$$

$$\psi(x, y, 0) = 0 \quad \text{for} \quad x \geqslant 0 \quad -\infty < y < \infty, \tag{29}$$

where $Ra = K\rho g\beta(T_c - T_\infty)b/\alpha_f \nu$ is the Rayleigh number, $\lambda = a/b$ denotes the aspect ratio of the conducting plate, $k = k_s/k_f$ is the ratio of the thermal conductivities in the conducting solid and the porous medium, and $\Gamma = \gamma\alpha_s/\alpha_f$ is the product of the ratio of heat capacity, γ, of the saturated porous medium to that of the fluid and the ratio of the thermal diffusivities of the porous medium and the solid.

The physical quantities which are then of most interest are the dimensionless local Nusselt numbers at the conjugate boundary and the heated wall, given by:

$$Nu_b(y, t) = -\left(\frac{\partial \theta_f}{\partial x}\right)_{x=0} \quad |y| \leqslant \tfrac{1}{2},$$

$$Nu_w(y, t) = -k\left(\frac{\partial \theta_s}{\partial x}\right)_{x=-\lambda} \quad |y| \leqslant \tfrac{1}{2},$$

respectively, and the corresponding dimensionless average Nusselt numbers, given by:

$$\overline{Nu}_b(t) = \int_{-1/2}^{1/2} Nu_b \, dy \quad \overline{Nu}_w(t) = \int_{-1/2}^{1/2} Nu_w \, dy.$$

3. APPROXIMATE ANALYTICAL SOLUTION

Given the large number of parameters present in the problem, it is worth identifying parameter ranges for which simplifications arise, before resorting to a full numerical solution. In particular, we highlight two such scenarios, in both of which a boundary layer forms on the porous side of the conjugate boundary; first, we formulate as generally as possible, and then consider the cases in turn. Assuming the boundary layer to be of thickness $O([x])$ and the stream function of magnitude $O([\psi])$, with $y \sim O(1)$, then, under the boundary-layer assumption, (16) and (17) reduce, on setting:

$$x = [x]X \quad \psi = [\psi]\Psi,$$

to:

$$\frac{\partial^2 \Psi}{\partial X^2} = -\frac{Ra[x]}{[\psi]}\frac{\partial \theta_f}{\partial X}, \tag{30}$$

$$\Gamma[x]^2 \frac{\partial \theta_f}{\partial t} + Ra[x]^2\left(\frac{\partial \Psi}{\partial y}\frac{\partial \theta_f}{\partial X} - \frac{\partial \Psi}{\partial X}\frac{\partial \theta_f}{\partial y}\right) = \frac{\partial^2 \theta_f}{\partial X^2}; \tag{31}$$

thence, we will require $[\psi] = Ra[x]$ from equation (30), with $[\psi]$ and $[x]$ to be determined from equation (31).

3.1. Ra $\gg$ 1 *and* $\Gamma \ll$ Ra

In this parameter range, convection balances diffusion in the boundary layer in which case $[x] = Ra^{-1/2}$ and $[\psi] = Ra^{1/2}$, so that equations (30) and (31) reduce to:

$$\frac{\partial^2 \Psi}{\partial X^2} = -\frac{\partial \theta_f}{\partial X},$$

$$\frac{\partial \Psi}{\partial y}\frac{\partial \theta_f}{\partial X} - \frac{\partial \Psi}{\partial X}\frac{\partial \theta_f}{\partial y} = \frac{\partial^2 \theta_f}{\partial X^2},$$

provided that $t \gg \Gamma/Ra$, which, since $\Gamma \ll Ra$, is effectively for all $t > 0$. Thus, the temperature and velocity within the boundary layer adjust instantaneously to conditions in the conducting solid side of the conjugate boundary, and time-dependency in the porous medium arises only through the conjugate boundary temperature. If we proceed by considering the vertically averaged solid temperature, $\bar{\theta}_s$, given by:

$$\bar{\theta}_s(x, t) = \int_{-1/2}^{1/2} \theta_s(x, y, t)\, dy,$$

and the vertically averaged conjugate boundary temperature, $\bar{\theta}_b(t)$, where:

$$\bar{\theta}_b(t) = \int_{-1/2}^{1/2} \theta_s(0, y, t)\, dy,$$

equation (18) reduces to:

$$\frac{\partial \bar{\theta}_s}{\partial t} = \frac{\partial^2 \bar{\theta}_s}{\partial x^2}, \tag{32}$$

subject to:

$$\bar{\theta}_s = 1 \quad \text{on} \quad x = -\lambda, \tag{33}$$

$$\bar{\theta}_s = \bar{\theta}_b(t) \quad \text{on} \quad x = 0, \tag{34}$$

and:

$$\frac{\partial \bar{\theta}_s}{\partial x} = -\frac{0.888[\bar{\theta}_b(t)]^{3/2}\, Ra^{1/2}}{k} \quad \text{on} \quad x = 0. \tag{35}$$

In particular, the last equation makes use of the result that:

$$\overline{Nu}_b(t) \approx 0.888[\bar{\theta}_b(t)]^{3/2}\, Ra^{1/2},$$

obtained by Vynnycky and Kimura [3], in conjunction with Cheng and Minkowycz [2]; this constitutes the time-dependent generalization of the result obtained in ref. [3], which is made permissible by the assumption that the porous medium boundary layer adjusts instantaneously to the solid plate temperature at each value of t, with $\theta_b(t)$ as the *a priori* unknown boundary temperature which must be solved for as part of the problem. By making the scalings $x = \lambda\tilde{x}$, $t = \lambda^2\tilde{t}$, equations (32)–(35) may then, on dropping the tildes, be reduced to their simplest form:

$$\frac{\partial \bar{\theta}_s}{\partial T} = \frac{\partial^2 \bar{\theta}_s}{\partial X^2}, \tag{36}$$

$$\bar{\theta}_s = 1 \quad \text{on} \quad X = -1, \tag{37}$$

$$\frac{\partial \bar{\theta}_s}{\partial X} = -\sigma \bar{\theta}_s^{3/2} \quad \text{on} \quad X = 0, \tag{38}$$

where σ ($= 0.888\lambda Ra^{1/2}/k$) is analogous to the Biot number which often occurs in conduction studies [11]. This is a straightforward diffusion equation for $\bar{\theta}_s$ which may be solved for $\sigma > 0$ using a Crank–Nicolson technique with iteration to take account of the non-linear boundary condition (38); the particular non-conjugate case when $\sigma = 0$ corresponds physically to a suddenly heated, and subsequently isothermal, plate with infinitesimal thickness, as considered previously by Ingham and Brown [9]. A further point worthy of note is the existence of a unique steady-state solution to these equations, given by:

$$\bar{\theta}_s(X) = (\bar{\theta}_b - 1)X + \bar{\theta}_b, \tag{39}$$

where:

$$\bar{\theta}_b = \begin{cases} \dfrac{1}{9\sigma^2}[(\phi + \sqrt{\phi^2 - 1})^{1/3} + (\phi + \sqrt{\phi^2 - 1})^{-1/3} - 1]^2 \\ \text{if } \sigma \geqslant \dfrac{2}{\sqrt{27}}, \\ \dfrac{1}{9\sigma^2}[2\cos(\frac{1}{3}\cos^{-1}(\phi)) - 1]^2 \quad \text{if } \sigma < \dfrac{2}{\sqrt{27}}, \end{cases} \tag{40}$$

where $\phi = (27\sigma^2/2) - 1$, as derived by Vynnycky and Kimura [3]; moreover, this indicates that, in the limit as $t \to \infty$, the present time-dependent formulation is indeed consistent with the time-independent solution of the earlier paper.

3.2. $\Gamma \gg 1$ *and* Ra $\ll \Gamma$

In this case, the transient term balances the diffusion term in equation (31), so it is appropriate to take $[x] = \Gamma^{-1/2}$, $[\psi] = Ra\,\Gamma^{-1/2}$, provided that $t \ll \Gamma/Ra$, corresponding physically to the case where conduction dominates convection in the early stages of the flow. On introducing the vertically averaged porous medium temperature, $\bar{\theta}_f$, given by:

$$\bar{\theta}_f(x, t) = \int_{-1/2}^{1/2} \theta_f(x, y, t)\, dy,$$

equations (30) and (31) reduce to:

$$\frac{\partial^2 \Psi}{\partial X^2} = -\frac{\partial \bar{\theta}_f}{\partial X}, \tag{41}$$

$$\frac{\partial \bar{\theta}_f}{\partial t} = \frac{\partial^2 \bar{\theta}_f}{\partial X^2}, \tag{42}$$

$$\frac{\partial \bar{\theta}_s}{\partial t} = \frac{\partial^2 \bar{\theta}_s}{\partial x^2}, \tag{43}$$

with the boundary conditions pertinent to the boundary layer now being:

$$\bar{\theta}_s = \bar{\theta}_f \quad \text{on} \quad X = 0,$$

$$k\frac{\partial \bar{\theta}_s}{\partial x} = \Gamma^{1/2}\frac{\partial \theta_f}{\partial X} \quad \text{on} \quad X = 0,$$

$$\theta_f \to 0, \quad \frac{\partial \psi}{\partial x} \to 0 \quad \text{as} \quad X \to \infty.$$

With reference to Carslaw and Jaeger [12], we obtain:

$$\bar{\theta}_s(x,t) = \sum_{n=0}^{\infty} \mu^n \left\{ \operatorname{erfc}\left[\frac{(2n+1)\lambda + x}{2\sqrt{t}}\right] - \mu \operatorname{erfc}\left[\frac{(2n+1)\lambda - x}{2\sqrt{t}}\right]\right\}, \tag{44}$$

$$\bar{\theta}_f(X,t) = \frac{2k}{\Gamma^{1/2}+k} \sum_{n=0}^{\infty} \mu^n \operatorname{erfc}\left[\frac{(2n+1)\lambda + X}{2\sqrt{t}}\right], \tag{45}$$

and

$$\Psi(X,t) = \frac{2k}{\Gamma^{1/2}+k} \sum_{n=0}^{\infty} \mu^n \left(X \operatorname{erfc}\left[\frac{(2n+1)\lambda + X}{2\sqrt{t}}\right] + 2\left(\frac{1}{\pi}\right)^{1/2} \left\{ \exp\left(-\frac{(2n+1)^2\lambda^2}{4t}\right) - \exp\left(-\frac{[(2n+1)\lambda + X]^2}{4t}\right)\right\} - (2n+1)\lambda \left\{ \operatorname{erf}\left[\frac{(2n+1)\lambda + X}{2\sqrt{t}}\right] - \operatorname{erf}\left[\frac{(2n+1)\lambda}{2\sqrt{t}}\right]\right\}\right), \tag{46}$$

where $\mu = (\Gamma^{1/2}-k)/(\Gamma^{1/2}+k)$, and erf (X) denotes the error function given by:

$$\operatorname{erf}(X) = \frac{2}{\sqrt{\pi}} \int_0^X \exp(-s^2)\,ds,$$

and erfc $(X) = 1 - \operatorname{erf}(X)$. Thence, we obtain the conjugate boundary temperature as:

$$\bar{\theta}_b(t) = \frac{2k}{\Gamma^{1/2}+k} \sum_{n=0}^{\infty} \mu^n \operatorname{erfc}\left[\frac{(2n+1)\lambda}{2\sqrt{t}}\right], \tag{47}$$

with the Nusselt number at the conjugate boundary as:

$$\frac{\partial \bar{\theta}_f}{\partial X} = -\frac{2k}{(\Gamma^{1/2}+k)\sqrt{\pi t}} \sum_{n=0}^{\infty} \mu^n \exp\left(-\frac{(2n+1)^2\lambda^2}{4t}\right), \tag{48}$$

and the heat flux at the fixed temperature boundary as:

$$k\frac{\partial \bar{\theta}_s}{\partial x} = -\frac{2k}{(\Gamma^{1/2}+k)\sqrt{\pi t}} \sum_{n=0}^{\infty} \mu^n \exp\left(-\frac{n^2\lambda^2}{t}\right). \tag{49}$$

Of note here is the fact that, although ψ depends on Ra, $\bar{\theta}_f$ does not, as might be expected since heat flow in the early stages is dominated by conduction rather than convection.

4. NUMERICAL SOLUTION

The partial differential equations (16)–(18) were finite-differenced using a control volume approach and non-uniform grid network as described by Patankar [13]. The details are essentially the same as those described in Vynnycky and Kimura [3], except for the inclusion of fully-implicit stepping for the time dependency in the problem; this amendment is relatively straightforward, and we therefore refer to the earlier paper for a complete validation of the method. In all cases, integration was carried out for unit aspect ratio, λ, until $t = 10$ using a time interval of 0.01; as might have been expected from equation (18), for $\Gamma \leqslant 10$, the integration time used proved sufficient to produce a steady state. We mention in passing that grid refinement was necessary in both x- and y-directions in the vicinity of the conjugate boundary: parallel to the plate in order to resolve the boundary layer that forms for $Ra \gg 1$, as well to take account accurately of the conjugate boundary condition, and along the plate, particularly in the vicinity of the leading edge at $y = -\frac{1}{2}$ in order to take account of the $(y+\frac{1}{2})^{-1/2}$ singularity in $\partial\theta_f/\partial x$ that arises there for $Ra \gg 1$. In addition, as was justified in ref. [3], the extent of the computational domain in the x- and y-directions, X_∞ and Y_∞, respectively, was taken to be $X_\infty = Y_\infty = 5$.

Our computations focused on those cases where a direct comparison with the simpler solutions of Section 3 was possible. In order to facilitate comparison, we use the layout of the previous section to analyse the results in two stages, depending on whether $Ra \gg 1$ and $\Gamma \ll Ra$, or $\Gamma \gg 1$ and $Ra \ll \Gamma$.

4.1. Ra $\gg$ 1 *and* $\Gamma \ll$ Ra

Figures 2 and 3 represent the streamline and isotherm development, respectively, for flow in the case when $\sigma = 25$ and $Ra = 500$; in both cases, the upper plots, labelled (a), represent the time evolution for the case when $\Gamma = 0$, and the lower ones, labelled (b), when $\Gamma = 10^3$. From the (a) plots, it is clear that a steady state has already been established as early as $t = 2.5$. The (b) plots, on the other hand, exhibit gradual development towards a steady state, which is still

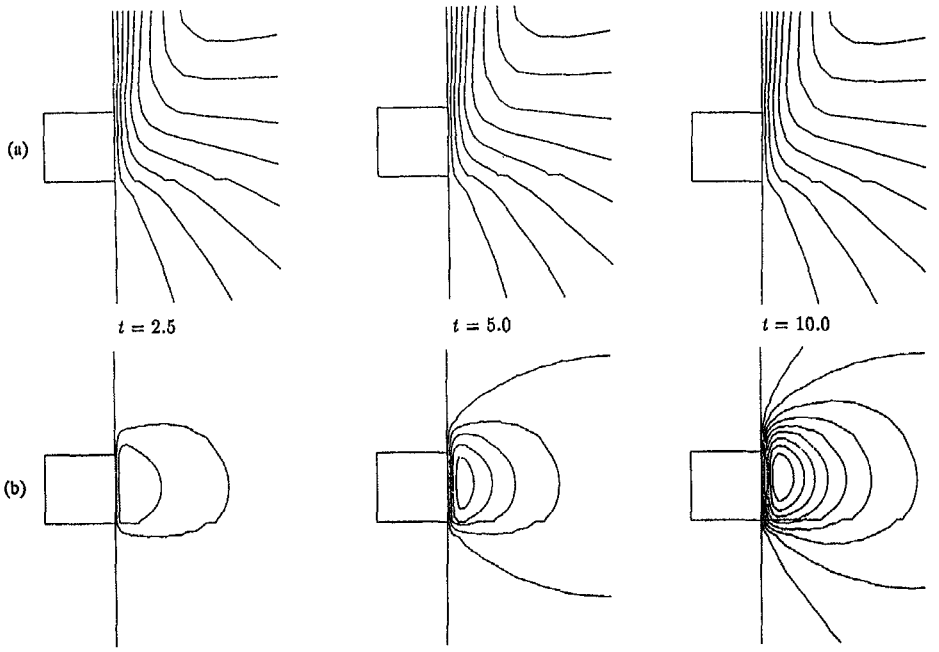

Fig. 2. Streamlines for $\sigma = 25$, $Ra = 500$ at $t = 2.5$, 5.0 and 10.0: (a) $\Gamma = 0$ ($\Delta\psi = 2.0$); (b) $\Gamma = 10^3$ ($\Delta\psi = 0.3$).

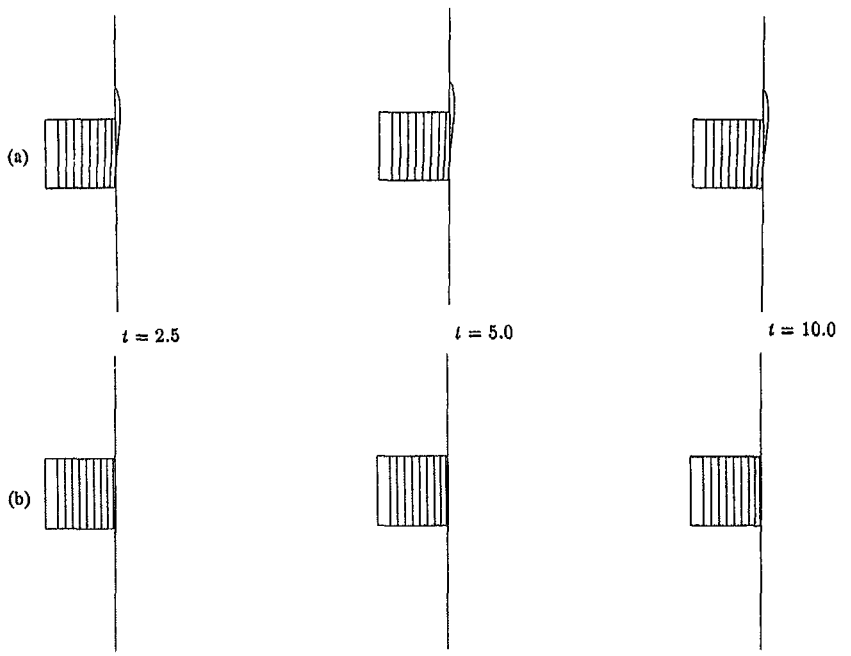

Fig. 3. Isotherms for $\sigma = 25$, $Ra = 500$ at $t = 2.5$, 5.0 and 10.0 ($\Delta\theta = 0.1$): (a) $\Gamma = 0$; (b) $\Gamma = 10^3$.

a long way off even at $t = 10$; by this stage, most of the temperature drop occurs across the solid plate, and the porous medium has not been warmed appreciably much above its initial temperature. Furthermore, Fig. 2(b) illustrates how the fluid flow is initiated once heating begins, namely by the establishment of a recirculating region which gradually expands and breaks to produce the streamline pattern of Fig. 2(a), wherein buoyancy forces transport fluid upwards once the porous medium has been sufficiently warmed.

A direct comparison with the analytical results of Section 3 is provided in Figs. 4–6 which illustrate, respectively, the average conjugate boundary temperature, the average conjugate boundary Nusselt number and the average heated wall Nusselt number for $\sigma = 0.25$, 2 and 25, $\Gamma = 0$, 10 and 10^3 when

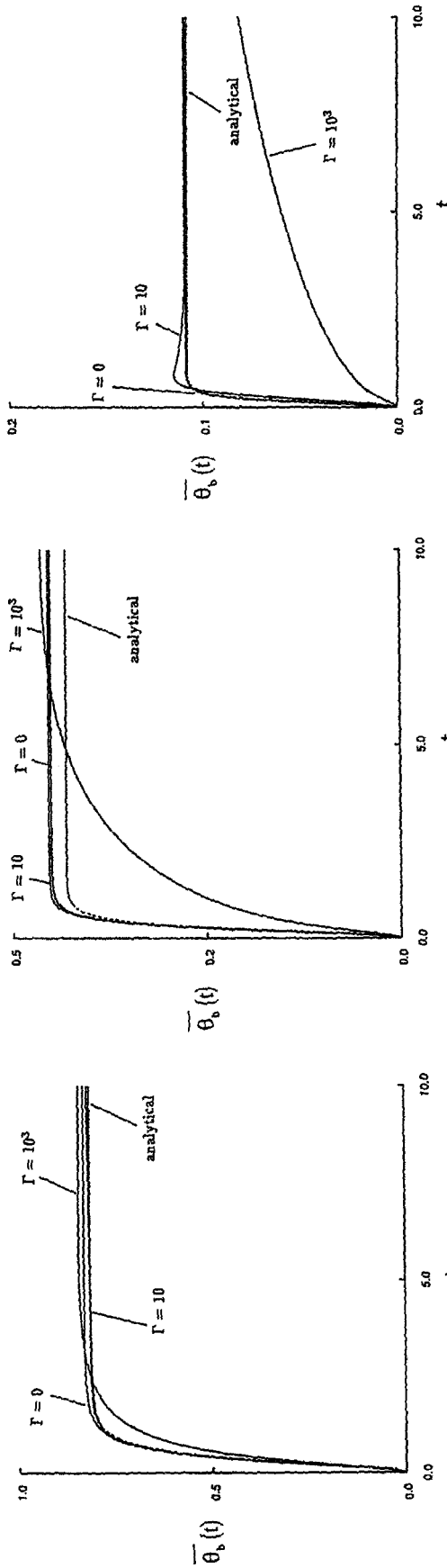

Fig. 4. Average conjugate boundary temperature $[\overline{\theta}_b(t)]$ vs time (t) with $Ra = 500$ ($\Gamma = 0$, 10 and 10^3) for: (a) $\sigma = 0.25$; (b) $\sigma = 2$; (c) $\sigma = 25$.

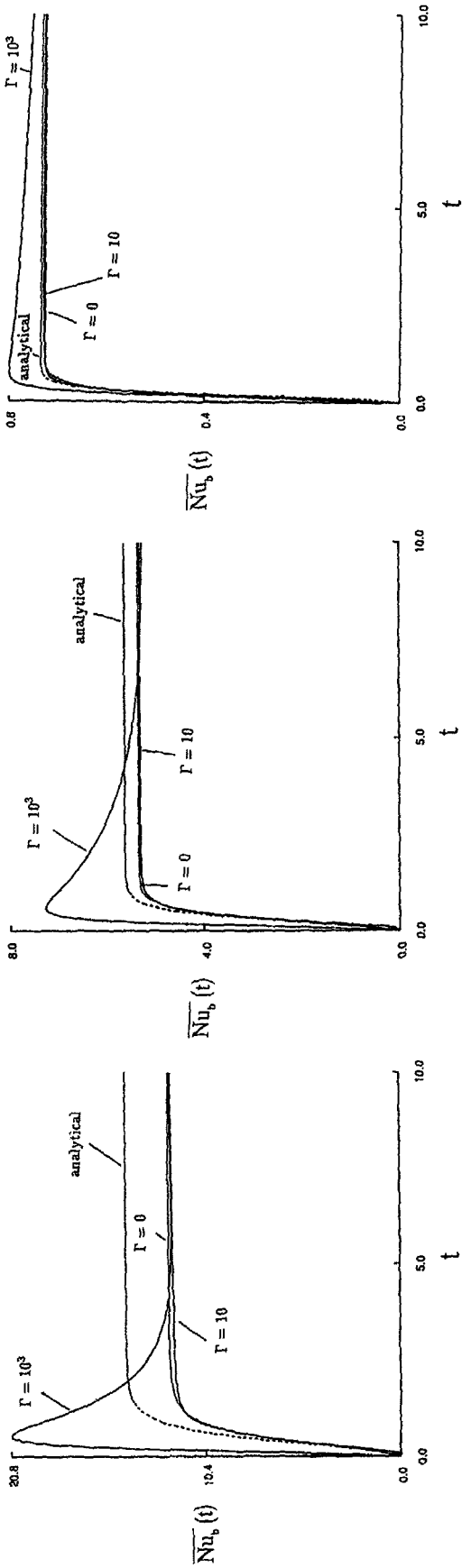

Fig. 5. Average conjugate boundary Nusselt number $[\overline{Nu_b}(t)]$ vs time (t) with $Ra = 500$ ($\Gamma = 0$, 10 and 10^3) for: (a) $\sigma = 0.25$; (b) $\sigma = 2$; (c) $\sigma = 25$.

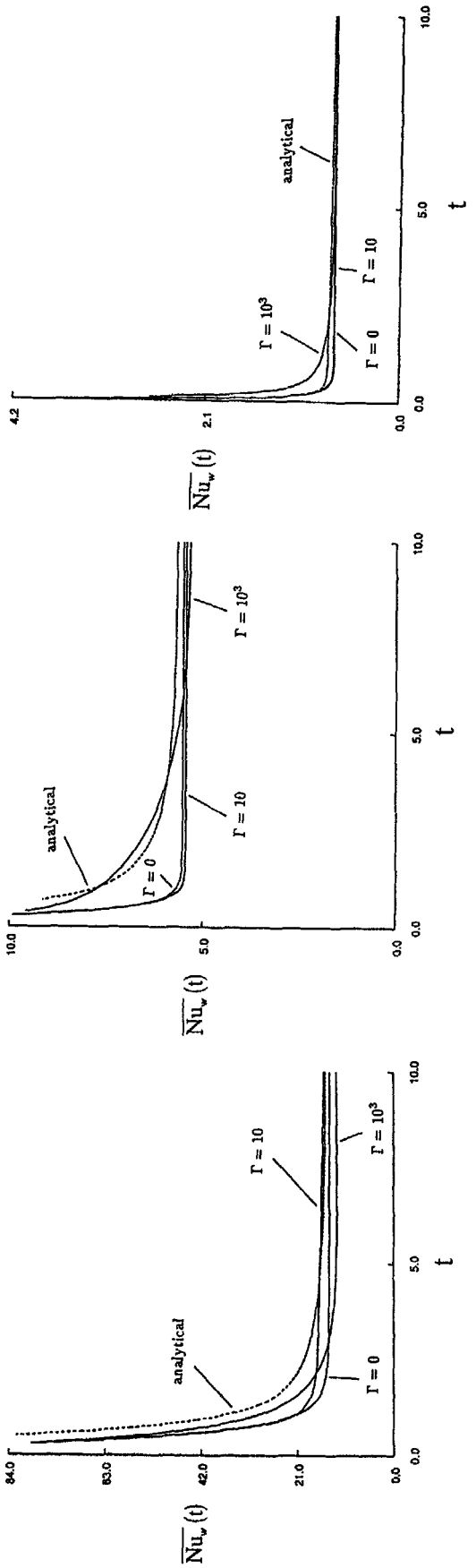

Fig. 6. Average heated wall Nusselt number $[\overline{Nu_w(t)}]$ vs time (t) with $Ra = 500$ ($\Gamma = 0$, 10 and 10^3) for: (a) $\sigma = 0.25$; (b) $\sigma = 2$; (c) $\sigma = 25$.

$Ra = 500$; $\Gamma = 10^3$ does not, of course, lie in the range of validity of the analytical solution (given by the dashed line), and hence agreement is expected to be poor, but it is included here in order to enable us to illustrate the heat transfer characteristics for a wide range of Γ when $Ra \gg 1$. In general, the agreement with the analytical solution for $\Gamma = 0$ and 10 is good for the average conjugate boundary temperature for all values of σ; as for the wall Nusselt numbers, this tends to be quite poor for $\sigma = 0.25$ [Figs. 5(a) and 6(a)], but improves with increasing σ: Figs. 5(c) and 6(c) for $\sigma = 25$ indicate excellent agreement for all values of t. The interaction of σ and Γ, as shown for example by Fig. 4(a)–(c) is also intriguing. Although for lower values of Γ, σ plays no role in determining how rapidly a steady state is reached, it is clear that, for $\Gamma = 10^3$, σ is the influential factor in governing the evolution rate; physically, this may be interpreted as the statement that a high value of σ, corresponding to a low thermal conductivity ratio, inhibits the rate of heat transfer to the porous medium, thence slowing the rate of growth of the conjugate boundary temperature. One other feature which merits attention is the overturn in the average conjugate boundary Nusselt number in Fig. 5(a) and (b): the combination of high conductivity ratio and high porous medium heat capacity ratio implies a sudden, initially high heat transfer rate at the conjugate boundary, before the Nusselt number stabilises.

4.2. $\Gamma \gg 1$ *and* $\mathrm{Ra} \ll \Gamma$

Figures 7 and 8 represent the streamline and isotherm development, respectively, for flow in the case when $k = 10$ and $\Gamma = 10^3$; in both cases, the upper plots, labelled (a), represent the time evolution for the case when $Ra = 100$, and the lower ones, labelled (b), when $Ra = 500$. In both cases, the choice of such a high value for Γ inevitably means for the plots shown, as $t = 2.5$, 5.0 and 10.0, that a steady state has yet to develop; the Rayleigh number clearly has no effect on the rate of evolution of a steady state, but merely determines the vigour of the stirring in the early stages of the flow, as well as governing the efficacy of heat transfer away from the conjugate boundary in a vertical plume adjacent to the wall. The physical interpretation of these plots is similar to that for Figs. 2(b) and 3(b); in particular, comparison of these figures with Figs. 7(b) and 8(b), for which $Ra = 500$ and $\Gamma = 10^3$ in both cases indicates the effect of an order of magnitude increase in k [since k $(= 0.888Ra^{1/2}/\sigma) \sim 1$ in the earlier figures], namely more effective heat transfer to the porous medium, as evidenced by the higher temperatures at the conjugate boundary.

Figures 9–11 serve to indicate the reliability of the analytical solution derived in Section 3.2 in comparison with the numerical computations; in all cases, the (a) plots represent results for $\Gamma = 10^2$, the (b) plots those for $\Gamma = 10^3$, and we note that, since from equations (47)–(49), $\bar{\theta}_b(t)$, $\overline{Nu}_w(t)$ and $\overline{Nu}_b(t)$ are independent of Ra, only one curve pertaining to the analytical solution is required in each case. As one would expect, the (a) plots give very poor agreement with the computed results, since the condition $\Gamma \gg Ra$ does not hold; the (b) plots, on the other hand, provide very good agreement for the case $Ra = 100$, which inevitably deteriorates for $Ra = 500$. A final point worthy of mention here is that around $t = 10$, there appear to be the first signs of divergence of the analytical solution from the numerical; the error at this stage is still, percentage-wise, relatively small, and so this observation is not out of step with the earlier remark that the analytical solution is valid provided $t \ll O(\Gamma/Ra)$.

5. CONCLUSIONS

We have considered the problem of transient conjugate free convection due to a heated vertical plate adjacent to a semi-infinite porous medium. By solving the heat and transfer equations numerically using finite differences, it has been possible to provide a detailed description of the effect of non-dimensional parameters such as the Rayleigh number (Ra), the ratio of the thermal conductivities (k), the plate aspect ratio (λ), the ratio of heat capacity (γ) of the saturated porous medium to that of the fluid and the ratio of the thermal diffusivities. In particular, the identification of the dimensionless parameter $\Gamma\,(= \gamma\alpha_s/\alpha_f)$ led us to consider two particular parameter ranges: $Ra \gg 1$ and $\Gamma \ll Ra$, and $\Gamma \gg 1$ and $Ra \ll \Gamma$. In both cases, analytic simplifications result in an altogether simpler formulation, giving equations whose solution proves to be more easily tractable than that of the original formulation; the case when $Ra \gg 1$ and $\Gamma \ll Ra$ corresponds to vigorous convective flow which settles down within an $O(1)$ time-scale to the steady state considered previously by Vynnycky and Kimura [3], whilst the case when $\Gamma \gg 1$ and $Ra \ll \Gamma$ corresponds to the situation where conduction dominates convection in the porous medium, as might occur in the early stages of flow development from zero initial conditions. In relation to this, it proves convenient to express our findings on a plot of Ra vs Γ, as in Fig. 12, indicating qualitatively the domains of validity of the analytical solutions, as well as the locations in (Γ, Ra) parameter space of our full numerical solutions. Agreement between the analytic and numerical solutions for the two regimes mentioned above proved to be good, leading us to believe that the analytical approach, although simple in nature, and hence computationally cheap, was successful in capturing the essential features of the heat transfer characteristics.

Computations executed outside the range of validity of the analytical solution shed light on several other interesting points. It was noted that, for the $Ra \gg 1$ regime, the rate of approach of the steady state for $\Gamma \gg 1$ was markedly accelerated by an increase in the thermal conductivity ratio, k. Furthermore, this also had the effect of producing an overturn in the

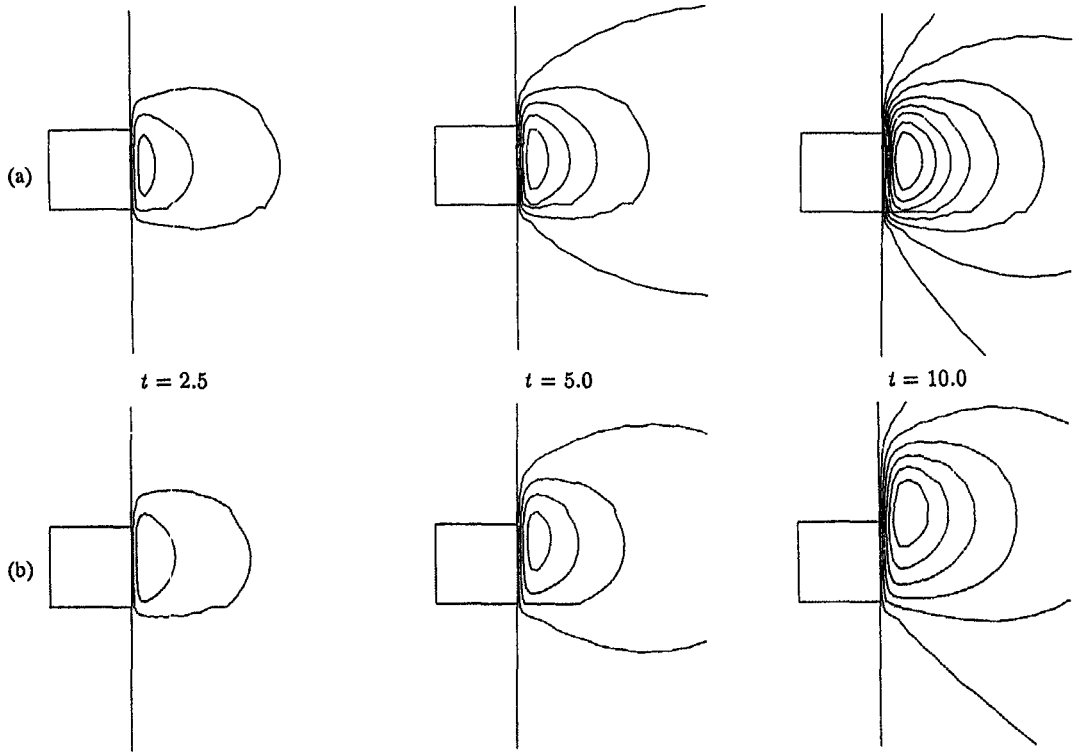

Fig. 7. Streamlines for $k = 10$, $\Gamma = 10^3$ at $t = 2.5$, 5.0 and 10.0: (a) $Ra = 100$ ($\Delta\psi = 0.5$); (b) $Ra = 500$ ($\Delta\psi = 3$).

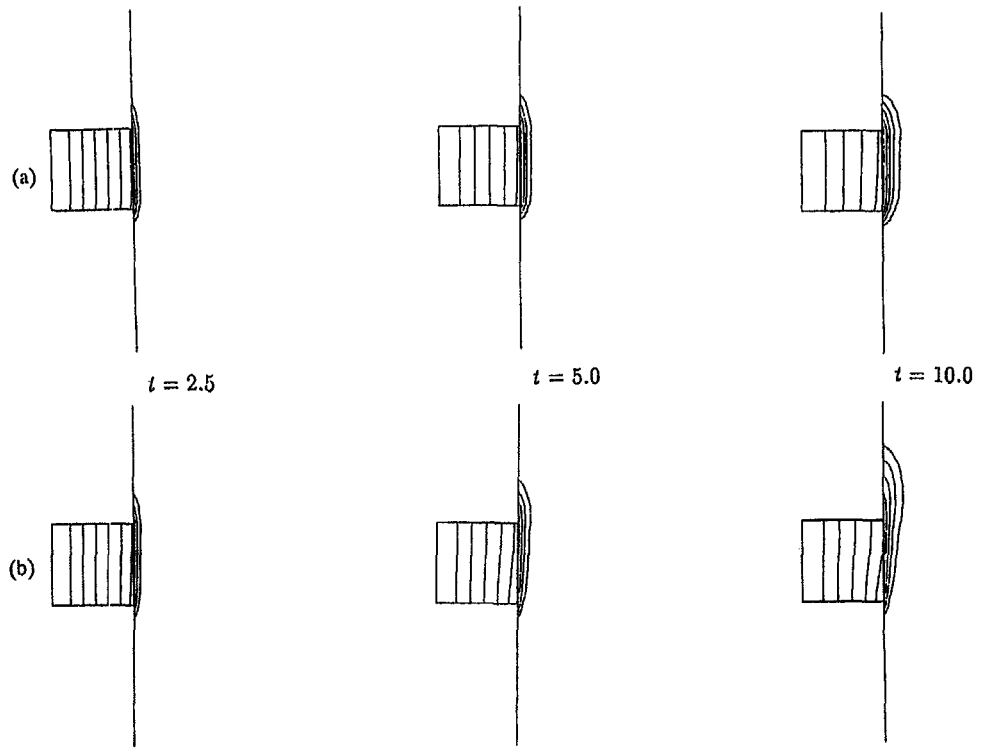

Fig. 8. Isotherms for $k = 10$, $\Gamma = 10^3$ at $t = 2.5$, 5.0 and 10.0 ($\Delta\theta = 0.1$): (a) $Ra = 100$; (b) $Ra = 500$.

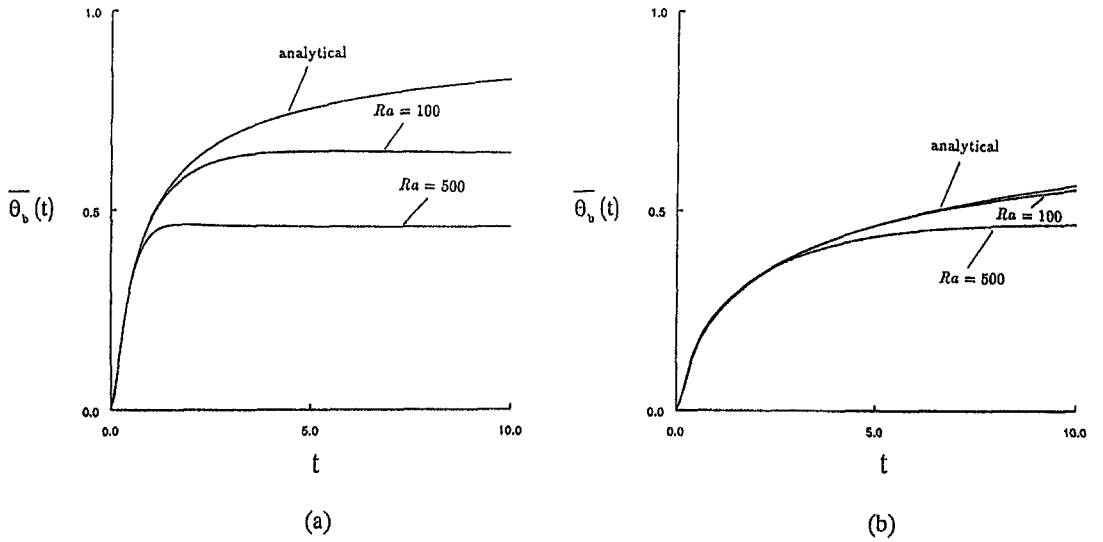

Fig. 9. Average conjugate boundary temperature $[\overline{\theta_b}(t)]$ vs time (t) with $k = 10$ ($Ra = 100$ and 500) for: (a) $\Gamma = 10^2$; (b) $\Gamma = 10^3$.

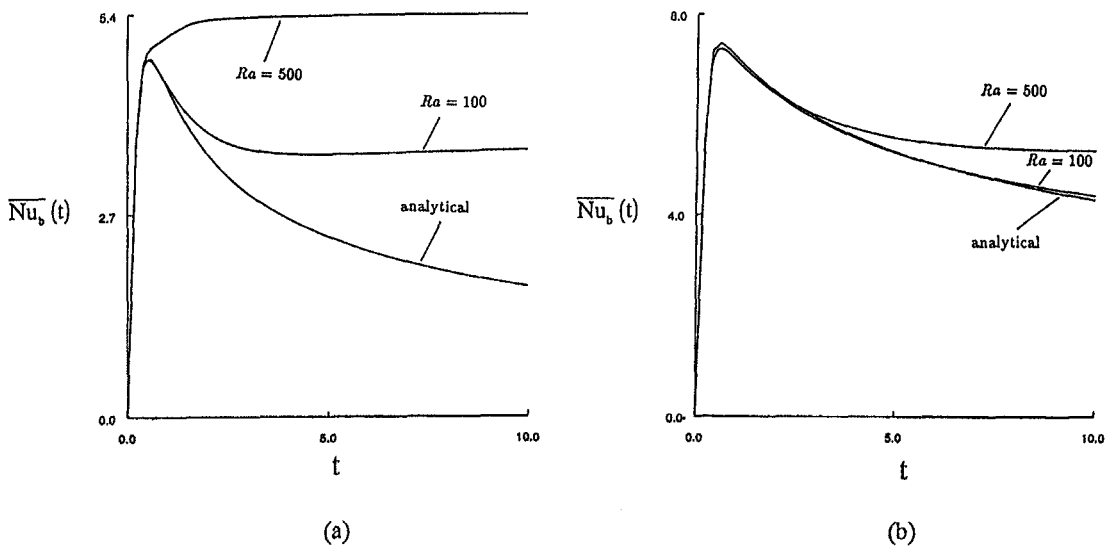

Fig. 10. Average conjugate boundary Nusselt number $[\overline{Nu_b}(t)]$ vs time (t) with $k = 10$ ($Ra = 100$ and 500) for: (a) $\Gamma = 10^2$; (b) $\Gamma = 10^3$.

average conjugate boundary Nusselt number during the early stages of the flow, in contrast to the monotonic progression to a steady state that occurred in both the numerical and analytical solutions for $\Gamma \approx O(1)$; on the other hand, the average heated wall Nusselt number for this parameter range indicates a uniform monotonic decrease to a steady state, at a rate much faster than that for the conjugate boundary. Although computations were executed for only one value of the aspect ratio, $\lambda (= 1)$, it may be plausible to suggest that the qualitative dependence of heat transfer characteristics on λ may be derived using the above and ref. [3].

A final remark concerns the actual number of relevant parameters and variables in the problem; from the foregoing, it is clear that in the general case the governing parameters are (Γ, Ra, k, λ), with (x, y, t) as the independent variables. However, previous studies for non-conjugate two-dimensional transient boundary-layer flow in a porous medium [9, 10] indicate the possibility of reducing the number of independent variables from three to two (η, τ say): for example, $\eta = x/y^{1/2}$, $\tau = t/y$ for the case when the heated plate is isothermal. For the present problem, however, a reduction to two independent variables, in the manner of refs. [9] and [10], seems possible only when $\sigma = 0$, in which case the solution of Ingham and Brown [9] for decay to a steady state when $\tau \gg 1$ would correspond to the $Ra \gg 1$, $Ra \gg \Gamma$, $t \gg \Gamma/Ra$ regime considered here in Section 3.1. On the other hand, it does

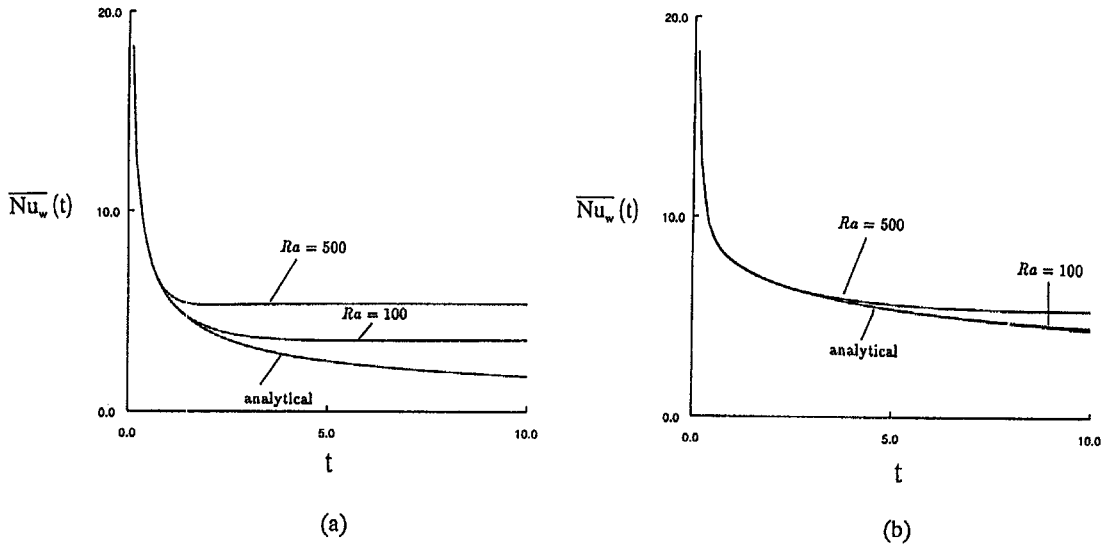

Fig. 11. Average heated wall Nusselt number $[\overline{Nu_w}(t)]$ vs time (t) with $k = 10$ ($Ra = 100$ and 500) for: (a) $\Gamma = 10^2$; (b) $\Gamma = 10^3$.

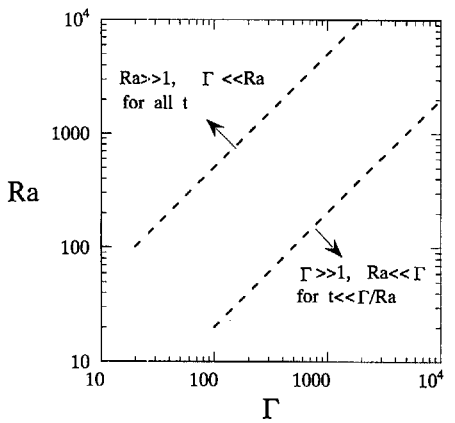

Fig. 12. Sketch of domains of validity for analytical solutions of Sections 3.1 and 3.2.

seem possible, in the limiting regimes identified in Section 3, to consider the problem wholly in terms of the three parameters $k/\Gamma^{1/2}$, $\lambda(Ra/\Gamma)^{1/2}$, Ra, with the time variable now taken to be $t(Ra/\Gamma)$. Consequently for $\Gamma \gg 1$, these parameters may be recovered explicitly by appropriate manipulation of the equations in Section 3.2; for $Ra \gg 1$, the situation is even simpler since two of the parameters combine to give σ, so that the problem depends only on Ra and σ.

Acknowledgement—The first author wishes to acknowledge the award of a fellowship from the Japanese Agency of Industrial Science and Technology.

REFERENCES

1. P. Cheng and I. Pop, Transient free convection about a vertical flat plate imbedded in a porous medium, *Int. J. Engng Sci.* **22,** 253–264 (1984).
2. P. Cheng and W. J. Minkowycz, Free convection about a vertical flat plate embedded in a porous medium with application to heat transfer from a dike, *J. Geophys. Res.* **82,** 2040–2044 (1977).
3. M. Vynnycky and S. Kimura, Conjugate free convection due to a vertical plate in a porous medium, *Int. J. Heat Mass Transfer* **37,** 229–236 (1994).
4. M. Vynnycky and S. Kimura, Conjugate free convection due to a heated vertical plate, submitted to *Numer. Heat Transfer* (1993).
5. S. Kimura and I. Pop, Conjugate free convection from a circular cylinder in a porous medium, *Int. J. Heat Mass Transfer* **35,** 3105–3113 (1992).
6. S. Kimura and I. Pop, Conjugate natural convection from a horizontal cylinder, *Numer. Heat Transfer* **25,** 347–361 (1993).
7. S. Kimura and I. Pop, Conjugate free convection from a sphere in a porous medium, *Int. J. Heat Mass Transfer* **37,** 2187–2192 (1994).
8. C. H. Johnson and P. Cheng, Possible similarity solutions for free convection boundary layers adjacent to flat plates in porous media, *Int. J. Heat Mass Transfer* **21,** 709–718 (1978).
9. D. B. Ingham and S. N. Brown, Flow past a suddenly heated vertical plate in a porous medium, *Proc. R. Soc. Lond. A* **403,** 51–80 (1986).
10. D. B. Ingham, J. H. Merkin and I. Pop, Flow past a suddenly cooled vertical flat surface in a saturated porous medium, *Int. J. Heat Mass Transfer* **25,** 1916–1919 (1982).
11. A. Bejan, *Convective Heat Transfer*. Wiley, New York (1984).
12. H. S. Carslaw and J. C. Jaeger, *Conduction of Heat in Solids* (2nd Edn). Clarendon Press, Oxford (1959).
13. S. V. Patankar, *Numerical Heat Transfer and Fluid Flow*. Hemisphere, Washington, DC (1980).